International Journal of Heat and Fluid Flow 45 (2014) 128–134

Contents lists available at ScienceDirect

International Journal of Heat and Fluid Flow

journal homepage: www.elsevier.com/locate/ijhff

Mechanism of drag reduction for circular cylinders with patterned surface

U. Butt *, L. Jehring, C. Egbers

Dept. of Aerodynamics and Fluid Mechanics, Brandenburg Univ. of Technology, Siemens-Halske-Ring 14, D-03046 Cottbus, Germany

ARTICLE INFO

Article history:
Received 4 October 2012
Received in revised form 22 October 2013
Accepted 25 October 2013
Available online 20 November 2013

Keywords:
Drag reduction
Flow control
Flow visualization

ABSTRACT

In this paper, the flow over cylinders with a patterned surface ($k/d = 1.98 \times 10^{-2}$) is investigated in a subsonic wind tunnel over Reynolds numbers ranging from 3.14×10^4 to 2.77×10^5 by measuring drag, flow visualization and measuring velocity profiles above the surface of the cylinders, to observe the effect of hexagonal patterns on the flow of air. These patterns can also be referred as hexagonal dimples or bumps depending on their configuration. The investigations revealed that a patterned cylinder with patterns pressed outwards has a drag coefficient of about 0.65 times of a smooth one. Flow visualization techniques including surface oil-film technique and velocity profile measurement were employed to elucidate this effect, and hence present the mechanism of drag reduction. The measurement of velocity profiles using hot-wire anemometry above the surface reveal that a hexagonal bump cause local separation generating large turbulence intensity along the separating shear layer. Due to this increased turbulence, the flow reattaches to the surface with higher momentum and become able to withstand the pressure gradient delaying the main separation significantly. Besides that, the separation does not appear to occur in a straight line along the length of the cylinder as in case of most passive drag control methods, but follow exactly the hexagonal patterns forming a wave with its crest at 115° and trough at 110°, in contrast to the laminar separation line at 85° for a smooth cylinder.

1. Introduction

Patterned steel sheets posses' better material properties such as tensile strength, and bending strength as compared to the plain sheets. Due to their known advantages, patterned pre-products exhibit a great potential to be manufactured with enhanced material properties besides weight reduction. To examine their possible application in Aerospace and automobile industry, aerodynamic properties of patterned pre-products must be investigated. The results are compared and assessed with respect to the commonly known structures i.e. dimples and roughened surfaces, whose characteristics are well documented in the literature. A quest for drag reduction and hence fuel consumption has always provoked researchers to look for new ways to achieve the goal. Investigations of flows over dimples (Bearman and Harvey, 1993; Bearman and Harvey', 1976), grooves (Aoki et al., 2009; Takayama and Aoki, 2005), screened surface (Oruc, 2012), rough surfaces (Achenbach, 1972, 1974), periodic blowing and suction from a slit on the sphere surface (Jeon et al., 2004) and surface trip wire (Maxworthy, 1969; Son et al., 2011) have proved to be much promising.

The mechanism of drag reduction due to surface roughness is thought to be caused by the transition from laminar to the turbulent boundary layer (Achenbach, 1974). As the turbulent boundary layer contains higher momentum the separation is delayed. The intriguing fact here is that the drag coefficient starts increasing after reaching its minimum at a critical Reynolds number (Fig. 1). The increase in the drag coefficient after reaching the critical Reynolds number is a result of an upstream shift of the separation line due to earlier growth of turbulent boundary layer.

Dimples and periodic blowing and suction follow the same drag reduction mechanism as drag-crisis mechanism, which is that the shear layer separated from the laminar boundary layer undergoes a transition to turbulence bringing high momentum towards the surface. As a result, the flow reattaches and becomes a turbulent boundary layer and the main separation is delayed (Choi et al., 2006). In contrast to the drag coefficient of the roughened surfaces, the change in drag coefficient of a dimpled cylinder is much smaller in the post critical regime (Fig. 1). As the infinitely long cylinders and spheres have the same value of critical Reynolds numbers and follow the same mechanism of drag crisis, with only exception that the flow over a sphere is three dimensional, investigations been carried out on dimpled spheres can also serve as a basis to comprehend the flow over dimpled cylinders. Choi et al. (2006) have explicitly explained the mechanism of drag reduction for a dimpled sphere by analyzing the boundary layer above the surface of the sphere. Accordingly, the generation of a separation bubble, i.e. a closed-loop streamline consisting of separation and

* Corresponding author. Tel.: +49 355 69 3427.
E-mail address: usman.butt@tu-cottbus.de (U. Butt).

0142-727X/$ - see front matter © 2013 Elsevier Inc. All rights reserved.
http://dx.doi.org/10.1016/j.ijheatfluidflow.2013.10.008

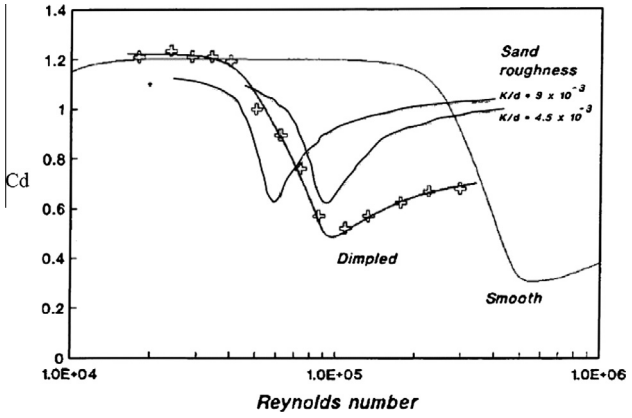

Fig. 1. Drag coefficient for smooth, dimpled, and roughened cylinders: smooth (Wieselberger, 1921); dimpled ($k/d = 9 \times 10^{-3}$) Bearman and Harvey, 1993; Sand roughened ($k/d = 9 \times 10^{-3}$, 4.5×10^{-3}) (Achenbach, 1971). Here k is the height of roughness or depth of dimples.

reattachment, on a body surface is an important flow-control strategy for drag reduction on a bluff body.

A 48% drag reduction for a cylinder by installing a much smaller cylinder in the upstream direction of the flow has been reported by Triyogi et al. (2009). The shear layer coming from the smaller cylinder changes the pressure distribution around the larger cylinder in such a way that the drag coefficient is dramatically altered. Takayama and Aoki (2005) show a clear reduction in drag of a cylinder with circular grooves having a depth to diameter ratio of 3.75×10^{-3}. Various qualitative flow visualization techniques such as smoke flow visualization and surface oil film technique as well as quantitative measuring techniques such as PIV have been employed to locate the position of transition and separation of boundary layers. Smoke flow visualization has been used by Bakic and Peric (2005) to visualize the delayed separation of the flow over a smooth sphere at Reynolds number of 4×10^5. Numerical investigations have also been very helpful in visualization of these complex flows over such structures. Yamagishi and Oki (2005) performed numerical investigations on the flow over grooved cylinders and have been able to locate exactly the position of boundary layer separation.

No studies have yet been made on the flow over cylinders with hexagonal patterns. Therefore, the presented results serve as a contribution for a better understanding of the described patterns, which can be referred as hexagonal dimples or bumps of $k/d = 1.98 \times 10^{-2}$, where k is the depth of the pattern. The behavior of the patterned cylinders for a particular range of Reynolds numbers is investigated in this paper using flow visualization, measuring their drag as well as the boundary layer velocity profiles above the cylinder surface. The evaluation of the measurement data supports the view of drag reduction due to patterned surfaces. The responsible mechanism is explained in detail in Section 3.4 considering the already known drag reduction mechanisms for dimples and rough surfaces.

2. Experimental setup

In this paper flow over cylinders with hexagonal patterns has been investigated. It is essential to mention here that these patterns were created on steel sheets with a smoothed surface to avoid any effects of surface roughness on the flow. Investigations were performed in a subsonic wind tunnel with an open test chamber. The motivation behind these tests was to study the effects of above mentioned hexagonal structures on the flow of air and their contribution in affecting the drag of the body. The cylinders to be investigated were made by bending and welding patterned steel sheets; firstly with the patterns facing outwards and secondly the patterns facing inwards. The orientation (Fig. 2) of these patterns towards the free stream of air was also changed during the Investigations, and hence the investigations could be performed over five different configurations. The length of the sheets required to form circular cylinders was calculated for a diameter of 156 mm through the formula $l = pi * D$ where D is the diameter of the cylinder and l the length of the sheet. A diameter D must be chosen that gives a length, which can be bent and welded together without distorting the continuity of the patterns on the line of joint. On the other hand, it can be stated confidently that a change in Reynolds number by defining the diameter by adding or subtracting the depths of the structures, which is 5.4%, is very small compared to the range of investigated Reynolds numbers.

All five investigated configurations have the following properties in Table 1.

The experiments were performed in a subsonic closed wind tunnel. The dimensions of the test chamber are $585 \times 585 \times 1300$ mm. The free stream turbulence intensity, defined as the ratio of root mean square of the velocity fluctuations to the mean velocity, is less than 0.5% for all experiments. The investigations were carried out for Reynolds numbers ranging from 3.14E+04 to 2.77E+05 based on cylinder diameter. The length of the cylindrical holder on which the test cylinder was mounted was made intentionally a little larger than the length of the test chamber to avoid three dimensional effects of finite cylinder length. Hence, the body can be considered as an infinitely long cylinder.

The total drag coefficient of the cylinder configuration was measured using a piezoelectric force gauge installed in a lever arm arrangement with its pivots hanging on cone edges. The cylinder and the sensor were attached on respective sides. The drag coefficient was measured with an uncertainty of ±9.2% at a measured force of 9.3 N and ±1.8% at a force of 180 N. Data were recorded at a rate of 4 values/s for a time period of 10 s. An average of all these measured values was taken.

The velocity profiles in the wake region of all the cylinder configurations were measured using hot wire anemometry. A single measurement was recorded for 15 s at a sampling rate of 10,000/s.

Two different flow visualization techniques were employed to investigate the flow and explicate the phenomenon of drag reduction. Oil-flow patterns were observed by applying the mixture of oil and titanium dioxide to the surface of cylinders. Silicon oil having a higher sheer force coefficient was chosen so that it can be pushed efficiently by the incoming free stream of air. Velocity profiles above the surface of cylinders were recorded using hot wire anemometry. A single hot wire probe was used for the measurements above the surface of the cylinders and an X-wire probe for the measurements in the wake region. The error for mean and r.m.s velocities was estimated to be ±4.3% and ±5.8% respectively.

3. Results and discussion

3.1. Drag variation

Fig. 3 shows the measured drag coefficients against Reynolds numbers for all the investigated configurations.

A data set of Cd vs Re is presented in Fig. 3 for Reynolds numbers $Re \leqslant 2.8 \times 10^5$, which is quiet below the critical Reynolds number of a smooth cylinder (Fig. 1). A significant reduction in drag coefficient can be seen for nearly all the configurations for higher Reynolds numbers with the largest drop for O90. A small increase in the Cd values for I0 and I90 at lower Re-numbers is also present. The Cd values of I90 rise initially a little higher than the smooth cylinder and drop slowly to a value close to the Cd value